

⁶⁸Ga-PRGD2 PET/CT in the Evaluation of Glioma: A Prospective Study

Deling Li,^{†,‡} Xiaobin Zhao,^{‡,§} Liwei Zhang,[†] Fang Li,[‡] Nan Ji,[†] Zhixian Gao,[†] Jisheng Wang,[†] Peng Kang,[†] Zhaofei Liu,[§] Jiyun Shi,[§] Xiaoyuan Chen,^{*,||} and Zhaohui Zhu^{*,‡}

[†]Department of Neurosurgery, Beijing Tiantan Hospital, Capital Medical University; China National Clinical Research Center for Neurological Diseases (NCRC-ND); Beijing Key Laboratory of Brain Tumor, Beijing, China

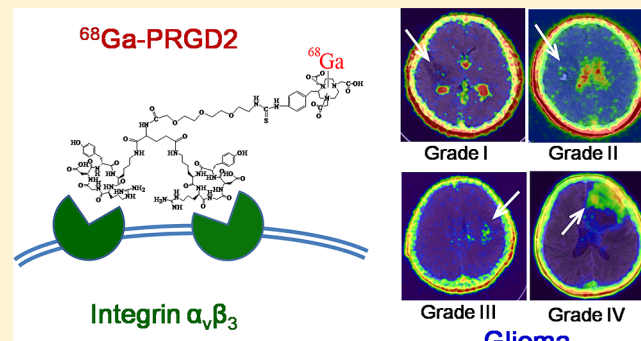
[‡]Department of Nuclear Medicine, Peking Union Medical College Hospital, Chinese Academy of Medical Sciences and Peking Union Medical College, Beijing, China

[§]Medical Isotopes Research Center, Peking University, Beijing, China

^{*}Laboratory of Molecular Imaging and Nanomedicine, National Institute of Biomedical Imaging and Bioengineering (NIBIB), National Institutes of Health (NIH), Bethesda, Maryland 20892, United States

ABSTRACT: Integrin $\alpha_v\beta_3$ is overexpressed in both neovasculature and glioma cells. We aimed to evaluate ⁶⁸gallium-BNOTA-PRGD2 (⁶⁸Ga-PRGD2) as a new reagent for noninvasive integrin $\alpha_v\beta_3$ imaging in glioma patients. With informed consent, 12 patients with suspicious brain glioma, as diagnosed by enhanced magnetic resonance imaging (MRI) scanning, were enrolled to undergo ⁶⁸Ga-PRGD2 PET/CT and ¹⁸F-FDG PET/CT scans before surgery. The preoperative images were compared and correlated with the pathologically determined WHO grade. Next, the expression of integrin $\alpha_v\beta_3$, CD34, and Ki-67 were determined by immunohistochemical staining of the resected brain tumor tissue. Our findings demonstrated that ⁶⁸Ga-PRGD2 specifically accumulated in the brain tumors that were rich of integrin $\alpha_v\beta_3$ and other neovasculature markers, but not in the brain parenchyma other than the choroid plexus. Therefore, ⁶⁸Ga-PRGD2 PET/CT was able to evaluate the glioma demarcation more specifically than ¹⁸F-FDG PET/CT. The maximum standardized uptake values (SUVmax) of ⁶⁸Ga-PRGD2, rather than those of ¹⁸F-FDG, were significantly correlated with the glioma grading. The maximum tumor-to-brain ratios (TBRmax) of both tracers were significantly correlated with glioma grading, whereas ⁶⁸Ga-PRGD2 seemed to be more superior to ¹⁸F-FDG in differentiating high-grade glioma (HGG) from low-grade glioma (LGG). Moreover, ⁶⁸Ga-PRGD2 PET/CT showed different accumulation patterns for HGG of WHO grades III and IV. This is the first noninvasive integrin imaging study, to the best of our knowledge, conducted in preoperative patients with different grades of glioma, and it preliminarily indicated the effectiveness of this novel method for evaluating glioma grading and demarcation.

KEYWORDS: integrin $\alpha_v\beta_3$, glioma, ⁶⁸Ga, PET/CT



INTRODUCTION

Gliomas are the most common malignant brain tumors, characterized by extensive, diffuse infiltrative growth into the surrounding brain parenchyma and different degrees of neovascularization.¹ Recent studies have demonstrated the diagnostic limitations of ¹⁸F-fluorodeoxyglucose (FDG) positron emission tomography (PET).² The diagnostic accuracy of ¹⁸F-FDG PET is weakened by high physiologic glucose metabolism in the brain areas where glioma is prone to occur, such as the cerebral cortex, basal ganglia, and thalamus. This significantly limited the sensitivity for glioma detection and the specificity for border demarcation. The uses of ¹¹C-methionine and ¹⁸F-fluorothymidine to image glioma showed better results but were still not enough for a final resolution.³ Thus, there is a need to develop a more specific radiotracer for PET to assess glioma.

Several researchers have demonstrated that the expression of the integrins $\alpha_v\beta_3$ and $\alpha_v\beta_5$, which are expressed in many glioma new-born vessels and glioma cells, generally increases with the grade of malignancy, and these integrins have been associated with poor prognosis,^{4,5} as replicated in a glioma animal model.⁶ Basic research showed that integrins could drive glioma progression⁷ and down-regulation of integrins or interference with integrin signaling pathways, which decreased migration and proliferation and improved survival in human glioblastoma cell lines.^{8,9} Cilengitide, an arginine-glycine-aspartic acid

Special Issue: Positron Emission Tomography: State of the Art

Received: April 30, 2014

Revised: July 31, 2014

Accepted: August 5, 2014

Published: August 5, 2014

(RGD) pentapeptide integrin $\alpha_5\beta_3$ and $\alpha_5\beta_5$ inhibitor, was shown to improve glioblastoma multiforme (GBM, WHO grade IV) prognosis, based on preclinical and current clinical trials assessing angiogenesis, cell invasion, and migration, and it has been investigated in combination with standard therapy in several clinical trials in GBM patients.^{10–14}

Glioma is known to be a highly heterogeneous disease, particularly regarding intratumoral heterogeneity, which contributes in part to drug resistance for some receptor inhibitors.¹⁵ Indeed, the premier research showed heterogeneous RGD uptake in GBM patients.¹⁶ With the advent of personalized medicine, understanding of intratumoral heterogeneity at different levels has become mandatory for improving clinical outcomes. Noninvasive RGD PET/CT imaging represents a more promising approach than ¹⁸F-FDG PET/CT for the specific visualization of integrin $\alpha_5\beta_3$ in preoperative glioma patients or for locating residual postoperative glioma; furthermore, this technique could potentially provide appropriate therapeutic guidance for anti-integrin targeted therapy and antiangiogenesis therapy, as well.

Until now, there have been only a small number of studies using RGD molecular imaging,^{6,17–20} including microPET studies, as well as studies using ^{99m}Tc-3P-RGD2 single-photon emission computed tomography/computed tomography (SPECT/CT) in subcutaneous tumor-bearing mice, MR relaxometry with RGD-labeled ultrasmall super paramagnetic iron oxide (USPIO), micro-SPECT/CT ^{99m}Tc-N₂S₂-Tat(49–57)-c(RGDyK) in cell lines and animal models, as well as ¹⁸F-RGD-K5 whole-body PET/CT in monkeys and human. Ji et al. demonstrated binding affinity against U87MG glioma cells by ^{99m}Tc-Galacto-RGD2, the tumor uptake of which was also in agreement with high integrin $\alpha_5\beta_3$ expression on glioma cells and in the neovasculature of nude mice bearing U87MG glioma xenografts.²¹

Schnell et al. reported the first clinical research about ¹⁸F-Galacto-RGD PET/CT scans in GBM patients.¹⁶ This study found that GBM demonstrated significant but heterogeneous RGD uptake, with the maximum uptake occurring in the highly proliferating and infiltrating areas of tumors, where $\alpha_5\beta_3$ expression was prominent in tumor microvessels, as well as in glial tumor cells. However, a limitation of this research was that it included not only newly diagnosed GBM but also recurrent GBM after external beam radiation or chemotherapy, thereby reducing its reliability.

In this prospective clinical study, we developed ⁶⁸gallium as a new positron emitter to label small RGD peptide antagonists of integrin $\alpha_5\beta_3$, and we investigated this emitter in a prospective clinical cohort covering patients with different grades of newly diagnosed brain glioma. We hypothesized that the integrin $\alpha_5\beta_3$ expression shown in ⁶⁸gallium-BNOTA-PRGD2 (⁶⁸Ga-PRGD2) PET/CT scans could more precisely predict the preoperative glioma grading and could determine the demarcation more specifically than ¹⁸F-FDG PET/CT scans. The results were compared with those generated with ¹⁸F-FDG PET/CT through clinical case-by-case evaluations.

MATERIALS AND METHODS

Patients. This study was approved by the Institute Review Boards of both Peking Union Medical College Hospital and Beijing Tiantan Hospital. It was conducted from November 2012 to March 2014. Written informed consent was obtained from all of the patients.

The inclusion criteria consisted of clinically based and magnetic resonance imaging (MRI)-based suspected newly diagnosed primary glioma; the patients were at least 18 years of age and had the ability to provide written and informed consent. The exclusion criteria were pregnancy, lactation, and inability to complete the needed examinations due to severe pain or claustrophobia. We evaluated all of the patients using preoperative brain ⁶⁸Ga-PRGD2 PET/CT and ¹⁸F-FDG PET/CT scans within 3 days. The pathology was determined by two neuropathologists separately, and they reached in consensus by referring a third pathologist when there was any discrepancy. The criteria of pathology diagnosis are the 2007 edition of WHO classification.²² Low-grade glioma (LGG) includes grades I–II, and high-grade glioma (HGG) includes grades III–IV. This study was registered at www.clinicaltrials.gov under number NCT01801371.

⁶⁸Ga-PRGD2 PET/CT Scanning. The cyclic RGD peptide was modified by PEGylated dimerization to form PEG3-E[c(RGDyK)]₂ (PRGD2) and was chelated with S-2-(4-isothiocyanatobenzyl)-1,4,7-triazacyclononane-1,4,7-triyltriacetic acid (BNOTA).^{23–25} ⁶⁸Ga-PRGD2 was synthesized on-site (immediately before injection) with radiochemical purity exceeding 97%. A Biograph 64 TruePoint TrueV PET/CT system (Siemens Medical Solutions, Erlangen, Germany) was used for scanning. For each patient, 1.85 MBq (0.05 mCi) of ⁶⁸Ga-PRGD2 per kilogram of body weight was injected intravenously. After 30 min of rest, the patients underwent the examinations. After a low-dose CT scan (120 kV, 35 mA, 3 mm layer, 512 × 512 matrix, 70 cm FOV), brain PET acquisition was performed (1 bed position, 10 min in duration).

¹⁸F-FDG PET/CT Scanning. The patients underwent brain ¹⁸F-FDG PET/CT within 3 days of the ⁶⁸Ga-PRGD2 PET/CT scan. ¹⁸F-FDG was produced on-site using Cyclotron RDS-111 (CTI, Knoxville, TN, USA). The same PET/CT system was used for scanning. Before the examinations, each patient was asked to fast for at least 4 h. The blood glucose levels of the patient were within normal limits (less than 6.4 mmol/L) before the ¹⁸F-FDG was injected at a dosage of 5.55 MBq (0.15 mCi) per kilogram of body weight. The patients rested quietly in a warm and dark room for approximately 1 h. Subsequently, the patients underwent the examinations, using the same parameters that had been employed for the ⁶⁸Ga-PRGD2 PET/CT scan.

Semiquantitative Analysis. Three experienced nuclear medicine physicians read all of the images through consensus reading. The same nuclear medicine physician examined and measured the semiquantitative values for the final analysis. A Siemens MMWP workstation was used for postprocessing. For each patient, the volume of interest (VOI) was drawn, and the maximum standardized uptake values (SUVmax) and maximum tumor-to-brain ratios (TBRmax) were recorded. TBRmax was obtained by dividing the SUVmax of the VOI by that of the unaffected contralateral brain.

Immunofluorescence and Immunohistochemical Analysis. We conducted the fluorescence staining to investigate integrin $\alpha_5\beta_3$ expression and immunohistochemical staining to see the angiogenesis of the patients and corroborated their PET/CT findings. Frozen tumor tissue sections were incubated with hamster antimouse integrin $\alpha_5\beta_3$ antibody (1:100; clone BV3, Abcam, USA) and Abegrin (10 µg/mL), and then visualized by Cy3-conjugated donkey antihamster secondary antibody (1:200; Jackson ImmunoResearch Laboratories) and FITC-conjugated donkey antihuman

Table 1. Demographic Characteristics of the Enrolled Patients with Glioma

no.	gender ^a	age (years)	surgery	WHO grading	pathology	location
1	F	23	craniotomy	I	dysembryoplastic neuroepithelial tumor	putamen, globus pallidus, insula
2	M	34	craniotomy	I	neuronal-glial tumor, focal forms, rosette-forming glioneuronal tumor	tegmentum of pons
3	M	40	craniotomy	I, focal II	mixed neuronal-glial tumors (oligoastrocytoma, dysembryoplastic neuroepithelial tumor)	frontal, temporal lobe
4	M	64	stereotactic biopsy	II	diffuse astrocytoma	frontal lobe, insula
5	M	51	craniotomy	II, focal III	oligoastrocytoma, focal anaplastic	temporal, parietal lobe
6	F	40	craniotomy	II, focal III	oligoastrocytoma, focal anaplastic	frontal, temporal lobe, insula
7	M	41	craniotomy	II, focal III	astrocytoma, focal anaplastic	temporal, parietal, occipital lobe
8	M	49	craniotomy	III, focal IV	anaplastic oligoastrocytoma, focal glioblastoma	parietal, occipital lobe
9	M	46	craniotomy	III, focal IV	anaplastic oligoastrocytoma, focal glioblastoma	frontal lobe
10	M	28	craniotomy	IV	glioblastoma	temporal lobe
11	M	66	craniotomy	IV	glioblastoma	frontal, temporal lobe
12	M	31	craniotomy	IV	glioblastoma	thalamus

^aM: male; F: female.

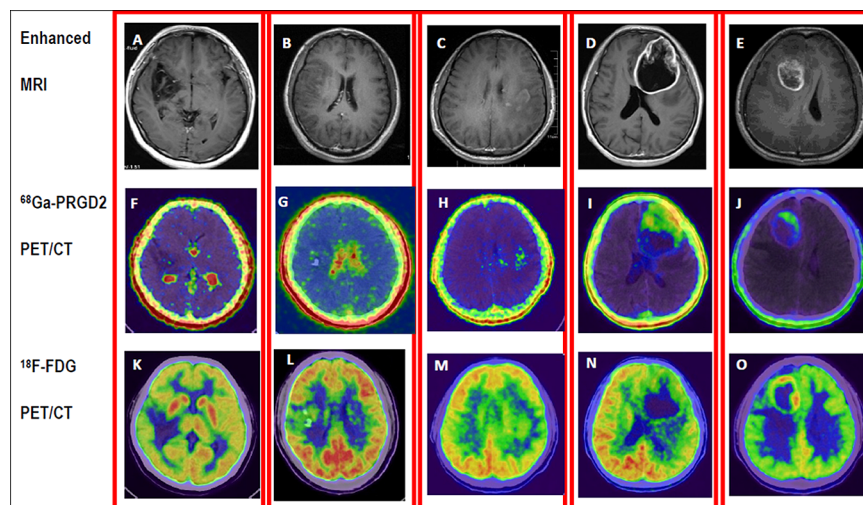


Figure 1. Demonstration of different WHO grade gliomas and comparison of the distribution of ⁶⁸Ga-PRGD2 and ¹⁸F-FDG in the tumors. Enhanced MRI (upper row) of five patients was obtained after administration of gadolinium contrast agent. Low-grade gliomas (LGG) (A/F/K: F, 23 y, grade I. B/G/L: M, 40y, grade II) showed void to minimal accumulation of ⁶⁸Ga-PRGD2 (middle row), whereas high-grade gliomas (HGG) (C/H/M: M, 41 y, grade III. D/I/N: M, 66 y, grade IV. E/G/O: M, 28 y, grade IV) showed moderate to intense uptake of ⁶⁸Ga-PRGD2. The high-level cortical accumulation deteriorated the value of ¹⁸F-FDG PET/CT (lower row) in grading and demarcation of glioma, especially the LGG.

secondary antibody (1:200) under the microscope (Carl Zeiss Axiovert 200M, Carl Zeiss, Thornwood, NY). Cryosections (4- μ m thick) were obtained and fixed in 95% ethanol for 10 min. Subsequently, 3% hydrogen peroxide (H_2O_2) was added to quench endogenous peroxidase, and 10% goat serum (Zsgb Bio, Beijing, China) was used to block the remaining epitopes. Tissue slices were subsequently incubated at room temperature with one of the following monoclonal antibodies: CD34 (clone QBEnd/10, Leica Biosystems, Germany) at a dilution of 1:50 and Ki-67 (clone EPS, Epitomics, USA) at a dilution of 1:100. The samples were incubated with homologous secondary antibodies conjugated with horseradish peroxidase (HRP) for 60 min and with diaminobenzidine (DAB) (K4065, DAKO, USA) at a dilution of 1:20 under microscopic examination. Finally, the sections were counterstained with hematoxylin.

Statistical Analysis. All of the data are expressed as means and standard deviation (SD). Spearman's correlation coefficient was calculated to assess the correlations between the SUVmax

and TBRmax of ⁶⁸Ga-PRGD2 and the grading of the glioma. All of the statistical analyses were performed using GraphPad Prism software (version 5.01, GraphPad Software, Inc., CA, USA), and $p < 0.05$ was considered to be statistically significant.

RESULTS

Patient Characteristics. The inclusion criteria were fulfilled by 12 patients (2 women, 10 men) with a mean age of 43 ± 13 years (range, 23–66 years). All of the patients presented with short histories of clinical symptoms or with newly diagnosed neurological deficits underwent MRI with gadolinium-DTPA enhancement suggesting a diagnosis of glioma and were last confirmed as glioma by postoperative pathology. The tumors were located in one brain lobe in 2 patients, in two lobes in 7 patients, in three lobes in 1 patient, in the thalamus in 1 patient, and in the pons in 1 patient (Table 1).

Comparison of ^{68}Ga -PRGD2 and ^{18}F -FDG PET/CT Scans. ^{68}Ga -PRGD2 did not accumulate in normal brain tissue, including the white matter and cortical gray matter, with the exception of the choroid plexus. Therefore, it could determine the boundary of glioma, compared to the clean background in patients' brains (Figure 1I,J). In contrast, ^{18}F -FDG uptake in some HGG was less than that in normal gray matter. Thus, HGG lesions were defined as low FDG uptake areas, surrounded by the relatively high ^{18}F -FDG uptake of the normal brain tissue (Figure 1N). Therefore, ^{68}Ga -PRGD2 PET/CT scans had much higher sensitivity for detecting glioma and higher specificity for determining tumor demarcation, compared to ^{18}F -FDG PET/CT scans.

The ^{68}Ga -PRGD2 accumulation pattern was different in grade III and IV glioma patients, compared with ^{18}F -FDG uptake. For anaplastic astrocytoma (grade III), the ^{68}Ga -PRGD2 expression had its own characteristic scattered focal area, resembling snowflakes (Figure 1H), while its uptake in GBM (grade IV) had much greater density, with a large bolus of PRGD2 accumulation (Figure 1I,J). In ^{18}F -FDG PET/CT, only the necrotic center without tracer uptake was a clue to identify grade IV glioma (Figure 1N,O), while the tracer accumulation in the solid components of grades III and IV glioma may be similar (Figure 1M,N). Therefore, the accumulation shape and density could be clues for differentiating grade III and IV gliomas, which have completely different prognoses.

Correlation of PET/CT Images with Glioma Grading.

As shown in Table 2, the SUVmax and TBRmax of ^{68}Ga -

Table 2. Correlation between the Glioma Grading and the Uptake of ^{18}F -FDG and ^{68}Ga -PRGD2^a

no.	regarded WHO grading	^{68}Ga -PRGD2		^{18}F -FDG	
		SUVmax	TBRmax	SUVmax	TBRmax
1	I (LGG)	0.79	0.80	5.90	0.57
2	I (LGG)	0.34	2.00	11.04	1.38
3	II (LGG)	0.09	0.90	10.70	1.30
4	II (LGG)	0.04	2.00	6.39	0.93
5	III (HGG)	0.75	8.33	7.73	1.31
6	III (HGG)	0.23	4.60	16.82	1.43
7	III (HGG)	0.44	4.40	6.24	1.11
8	IV (HGG)	2.31	3.55	15.76	1.36
9	IV (HGG)	1.9	10.56	8.87	2.07
10	IV (HGG)	1.21	11.00	7.69	1.77
11	IV (HGG)	0.88	4.63	37.18	4.77
12	IV (HGG)	0.5	10.00	10.43	3.02
<i>r</i>		0.67	0.82	0.32	0.75
<i>p</i>		0.02*	0.001*	0.30	0.005*

^aRegarded WHO grading, the highest WHO grade of the total tumor when heterogeneity exists; SUV_{max}, maximal standardized uptake value; TBR_{max}, maximum tumor-to-background ratio; LGG, low-grade glioma; HGG, high-grade glioma; *r*, correlation coefficient to the regarded WHO grading. **p* < 0.05 was considered to be significant.

PRGD2 were significantly correlated with the glioma grading (*r* = 0.67, *p* = 0.02, and *r* = 0.82, *p* = 0.001, respectively). In this group of patients, the TBRmax of ^{18}F -FDG was significantly correlated with the glioma grading (*r* = 0.75, *p* = 0.005), whereas the SUVmax of ^{18}F -FDG was not correlated with the glioma grading (*r* = 0.32, *p* = 0.30). The TBRmax of ^{68}Ga -PRGD2 and ^{18}F -FDG were both significantly correlated with the glioma grading (Table 2). However, for differentiating the

HGG from the LGG, ^{68}Ga -PRGD2 PET/CT reached 100% (8/8) sensitivity and 100% (4/4) specificity in this small group of patients when the threshold of TBRmax was set between 2.00 and 3.55, whereas the sensitivity, specificity, and accuracy of ^{18}F -FDG PET/CT were 88% (7/8), 75% (3/4), and 83% (10/12), respectively, with the TBRmax threshold setting between 1.30 and 1.31.

Histopathological Features and Immunohistochemical Staining of Resected Tumor Tissue. Tumor pathology determination of each of 11 patients' tumors was conducted on total resections or gross resections, whereas one patient missed the analysis because he received only stereotactic biopsy for the unresectable diffuse growth of the tumor.

We examined the histopathology and expression of integrin $\alpha_3\beta_3$ in the brain tumor tissue of 11 patients to corroborate the relevant findings with the ^{68}Ga -PRGD2 PET/CT findings. In agreement with the intense ^{68}Ga -PRGD2 accumulation in HGG (Figure 1), high levels of integrin $\alpha_3\beta_3$ receptor were selectively expressed on the tumor cells of HGG (Figure 3B,F), comparing to extremely low expression of integrin $\alpha_3\beta_3$ in LGG (Figure 2D). An extensive vascular network, with ongoing

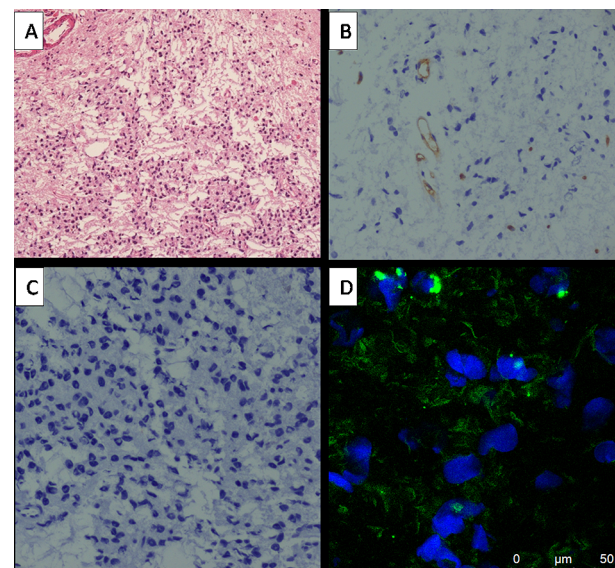


Figure 2. Immunohistochemical and immunofluorescence stains of the glioma of the patient (patient no. 1 Table 1, MRI and PET/CT images shown in Figure 1A,F,K) with LGG. (A) Hematoxylin-eosin staining showed WHO grade I glioma (magnification 100 \times). (B) The CD34 stains indicated few vascular networks in the tumors (magnification 200 \times). (C) Negative nuclear expression of KI-67 indicated low proliferation (magnification 200 \times). (D) Very low expression of the integrin $\alpha_3\beta_3$ receptor were observed in the tumor or vascular endothelial cells.

angiogenesis and proliferation, was observed in the HGG brain tumor tissue, as demonstrated by positive staining of CD34 (Figure 3C,G) and KI-67 (Figure 3D,H).

DISCUSSION

Over the past decade, numerous studies have demonstrated that ^{18}F -FDG PET/CT is helpful for assessing glioma grading, determining the anaplastic transformation of LGG, differentiating recurrent glioma and radiation necrosis, and even predicting the survival of patients with recurrent glioma.^{3,26–28} However, the sensitivity of glioma detection by ^{18}F -FDG PET/

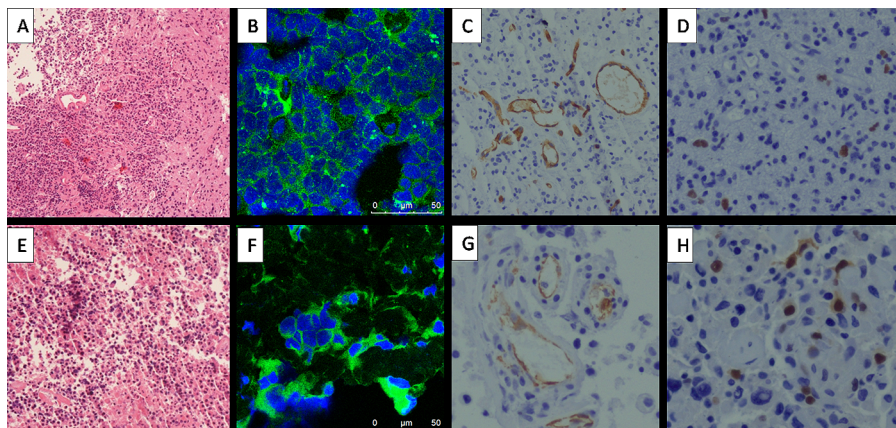


Figure 3. Immunohistochemical and immunofluorescence stains of the glioma of the patient (upper row A/B/C/D, patient no. 8 in Table 1; lower row E/F/G/H, patient no. 10 in Table 1; MRI and PET/CT images shown in Figure 1 E,G,O) with HGG. (A,E) Hematoxylin-eosin staining showed anaplastic oligoastrocytoma (WHO grade III) and GBM (WHO grade IV), respectively (magnification 100×). (B,F) High levels of expression of the integrin $\alpha_v\beta_3$ were observed in the tumor (magnification 200×). (C,G) The CD34 stains indicate more extensive vascular network in the tumors than that in Figure 2B (magnification 200×). (D,H) Positive nuclear expression of Ki-67 indicates active proliferation (magnification 200×).

CT is relatively low, particularly for LGG, because ^{18}F -FDG uptake in LGG is usually similar to that of normal white matter. Even in HGG, ^{18}F -FDG uptake varied greatly.²⁹ ^{18}F -FDG uptake, by assessing only the mechanisms associated with elevated glucose metabolism, is nonspecific for the molecular characteristics of glioma.

^{68}Ga -PRGD2 was specifically designed to target the endothelial cells of the neovasculature and glioma cells that express integrin $\alpha_v\beta_3$ at high levels in glioma. We demonstrated that the ^{68}Ga -PRGD2 PET/CT had higher sensitivity than ^{18}F -FDG due to the clear lack of ^{68}Ga -PRGD2 affinity of the normal brain.

SUVmax and TBR are both used to explain tumor PET/CT imaging, and they offer different advantages, with the former traditionally regarded as providing the representative value of each tumor. In this research, the SUVmax of ^{18}F -FDG was not correlated with glioma grading; one reason for this finding was that different patients' brains had different ^{18}F -FDG uptake backgrounds. In previous research, different regions of the brain have been used for reference uptake as the index of TBR in semiquantitative analysis, including white matter and unaffected contralateral gray matter. One study demonstrated that cutoff levels of 1.5 for the tumor-to-white matter (T/WM) FDG uptake ratio and 0.6 for the tumor-to-cortex (T/C) ratio were useful in the differentiation of LGG from HGG, with sensitivity of 94% and specificity of 77%.²⁸ However, TBRmax is more indicative of the most aggressive location in the tumor, and it can determine accurate grading for heterogeneous tumors. Additionally, it is easier and more reasonable to be used in clinical practice than the T/WM and T/C ratios because glioma can occur in both white matter and cortex, and it is sometimes difficult to distinguish the white matter and cortex on the CT images of PET/CT. Moreover, TBRmax has been increasingly used in new tracer PET/CT scans to assess glioma.^{30–32} The TBRmax values of ^{18}F -FDG and ^{68}Ga -PRGD2 PET/CT were both significantly correlated with glioma grading, but the former could not differentiate LGG from HGG, and it showed some overlap between these two groups of values. Therefore, ^{68}Ga -PRGD2 PET/CT was superior to ^{18}F -FDG in distinguishing LGG from HGG.

To the best of our knowledge, this was the first study conducted in humans that investigated the use of integrin imaging (specifically ^{68}Ga -PRGD2 PET/CT) for preoperative, noninvasive assessment of glioma grading. We compared the findings of this technique with ^{18}F -FDG PET/CT findings from the same patients. We provided histopathological confirmation showing that the different levels of expression of integrin $\alpha_v\beta_3$ on glioma cells corresponded to the WHO glioma grading.

There are some limitations of the present study. First, the number of enrolled patients with glioma was small, especially in the lower grade group. However, each patient underwent ^{68}Ga -PRGD2 PET/CT and ^{18}F -FDG PET/CT scanning, and the preliminary results of this study support a pilot proof-of-concept study. Second, the study lacked a sufficient number of control patients with other types of brain tumors. An additional study is required to recruit a broad variety of patients with brain-occupying lesions to determine the sensitivity, specificity, and accuracy of ^{68}Ga -PRGD2 PET/CT in assessing glioma. Studies with more cases are needed to correlate the imaging findings related to post-treatment changes with the clinical responses and final prognoses of patients with glioma.

In conclusion, this prospective clinical study demonstrated that ^{68}Ga -PRGD2 PET/CT is a specific method for identifying and assessing glioma neovasculature formation and glioma cells in patients with glioma. In contrast to ^{18}F -FDG PET/CT, ^{68}Ga -PRGD2 PET/CT is more specific for evaluating glioma demarcation. The SUVmax of ^{68}Ga -PRGD2 is significantly correlated with glioma grading, and the TBRmax of ^{68}Ga -PRGD2 is more superior to ^{18}F -FDG for differentiating HGG from LGG. Therefore, ^{68}Ga -PRGD2 PET/CT may be a useful tool for assessing glioma grading, demarcation, and neovasculature formation.

■ AUTHOR INFORMATION

Corresponding Authors

*(Z.Z.) Phone: 86-13611093752. E-mail: zhuzhh@pumch.cn.

*(X.C.) Phone: 301-451-4246. E-mail: shawn.chen@nih.gov.

Author Contributions

[†]These authors (D.L. and X.Z.) contributed equally to this work.

Notes

The authors declare no competing financial interest.

ACKNOWLEDGMENTS

This work was supported, in part, by National Key Scientific Instrument and Equipment Development Project (2011YQ17006710), Major State Basic Research Development Program of China (973 Program) (Grant Nos. 2013CB733802 and 2014CB744503), the National Natural Science Foundation of China projects (81171370, 81271614, and 81371596), the Capital Special Project for Featured Clinical Application (Z121107001012119), a Beijing Key Laboratory of Brian Tumor Project, and the Intramural Research Program (IRP), National Institute of Biomedical Imaging and Bioengineering (NIBIB), National Institutes of Health (NIH). The authors are grateful to Guijun Jia, Ming Ni, Lin Qiao, and the other related staff at Beijing Tiantan Hospital, who helped in performing this study and collecting the data. Also we thank Junmei Wang, Yun Cui, and Peng Zhang for immunohistochemical analysis.

REFERENCES

- (1) Plate, K. H.; Scholz, A.; Dumont, D. J. Tumor angiogenesis and anti-angiogenic therapy in malignant gliomas revisited. *Acta Neuropathol.* **2012**, *124* (6), 763–75.
- (2) la Fougere, C.; Suchorska, B.; Bartenstein, P.; Kreth, F. W.; Tonn, J. C. Molecular imaging of gliomas with PET: opportunities and limitations. *Neuro-Oncology* **2011**, *13* (8), 806–19.
- (3) Miyake, K.; Shinomiya, A.; Okada, M.; Hatakeyama, T.; Kawai, N.; Tamiya, T. Usefulness of FDG, MET and FLT-PET studies for the management of human gliomas. *J. Biomed. Biotechnol.* **2012**, *2012*, 205818.
- (4) Schittenhelm, J.; Schwab, E. I.; Serveslage, J.; Tatagiba, M.; Meyermann, R.; Fend, F.; Goodman, S. L.; Sipos, B. Longitudinal expression analysis of alphav integrins in human gliomas reveals upregulation of integrin alphavbeta3 as a negative prognostic factor. *J. Neuropathol. Exp. Neurol.* **2013**, *72* (3), 194–210.
- (5) Schnell, O.; Krebs, B.; Wagner, E.; Romagna, A.; Beer, A. J.; Grau, S. J.; Thon, N.; Goetz, C.; Kretzschmar, H. A.; Tonn, J. C.; Goldbrunner, R. H. Expression of integrin alphavbeta3 in gliomas correlates with tumor grade and is not restricted to tumor vasculature. *Brain Pathol.* **2008**, *18* (3), 378–86.
- (6) Shao, G.; Zhou, Y.; Wang, F.; Liu, S. Monitoring glioma growth and tumor necrosis with the U-SPECT-II/CT scanner by targeting integrin alphavbeta3. *Mol. Imaging* **2013**, *12* (1), 39–48.
- (7) Holmes, K. M.; Annala, M.; Chua, C. Y.; Dunlap, S. M.; Liu, Y.; Hugen, N.; Moore, L. M.; Cogdell, D.; Hu, L.; Nykter, M.; Hess, K.; Fuller, G. N.; Zhang, W. Insulin-like growth factor-binding protein 2-driven glioma progression is prevented by blocking a clinically significant integrin, integrin-linked kinase, and NF-kappaB network. *Proc. Natl. Acad. Sci. U.S.A.* **2012**, *109* (9), 3475–80.
- (8) Adachi, Y.; Lakka, S. S.; Chandrasekar, N.; Yanamandra, N.; Gondi, C. S.; Mohanam, S.; Dinh, D. H.; Olivero, W. C.; Gujrati, M.; Tamiya, T.; Ohmoto, T.; Kouraklis, G.; Aggarwal, B.; Rao, J. S. Down-regulation of integrin alpha(v)beta(3) expression and integrin-mediated signaling in glioma cells by adenovirus-mediated transfer of antisense urokinase-type plasminogen activator receptor (uPAR) and sense p16 genes. *J. Biol. Chem.* **2001**, *276* (50), 47171–7.
- (9) Koutsoumpa, M.; Polytarchou, C.; Courty, J.; Zhang, Y.; Kieffer, N.; Mikelis, C.; Skandalis, S.; Hellman, U.; Iliopoulos, D.; Papadimitriou, E. Interplay between alpha v beta 3 integrin and nucleolin regulates human endothelial and glioma cell migration. *J. Biol. Chem.* **2012**, *288*, 343–54.
- (10) Lomonaco, S. L.; Finniss, S.; Xiang, C.; Lee, H. K.; Jiang, W.; Lemke, N.; Rempel, S. A.; Mikkelsen, T.; Brodie, C. Cilengitide induces autophagy-mediated cell death in glioma cells. *Neuro-Oncology* **2011**, *13* (8), 857–65.
- (11) Gilbert, M. R.; Kuhn, J.; Lamborn, K. R.; Lieberman, F.; Wen, P. Y.; Mehta, M.; Cloughesy, T.; Lassman, A. B.; Deangelis, L. M.; Chang, S.; Prados, M. Cilengitide in patients with recurrent glioblastoma: the results of NABTC 03-02, a phase II trial with measures of treatment delivery. *J. Neurooncol.* **2012**, *106* (1), 147–53.
- (12) Nabors, L. B.; Mikkelsen, T.; Hegi, M. E.; Ye, X.; Batchelor, T.; Lesser, G.; Peereboom, D.; Rosenfeld, M. R.; Olsen, J.; Brem, S.; Fisher, J. D.; Grossman, S. A. A safety run-in and randomized phase 2 study of cilengitide combined with chemoradiation for newly diagnosed glioblastoma (NABTT 0306). *Cancer* **2012**, *118* (22), 5601–5607.
- (13) Scaringi, C.; Minniti, G.; Caporello, P.; Enrici, R. M. Integrin inhibitor cilengitide for the treatment of glioblastoma: a brief overview of current clinical results. *Anticancer Res.* **2012**, *32* (10), 4213–23.
- (14) MacDonald, T. J.; Vezina, G.; Stewart, C. F.; Turner, D.; Pierson, C. R.; Chen, L.; Pollack, I. F.; Gajjar, A.; Kieran, M. W. Phase II study of cilengitide in the treatment of refractory or relapsed high-grade gliomas in children: a report from the Children's Oncology Group. *Neuro-Oncology* **2013**, *15* (10), 1438–44.
- (15) Nathanson, D. A.; Gini, B.; Mottahedeh, J.; Visnyei, K.; Koga, T.; Gomez, G.; Eskin, A.; Hwang, K.; Wang, J.; Masui, K.; Paucar, A.; Yang, H.; Ohashi, M.; Zhu, S.; Wykosky, J.; Reed, R.; Nelson, S. F.; Cloughesy, T. F.; James, C. D.; Rao, P. N.; Kornblum, H. I.; Heath, J. R.; Cavenee, W. K.; Furnari, F. B.; Mischel, P. S. Targeted therapy resistance mediated by dynamic regulation of extrachromosomal mutant EGFR DNA. *Science* **2014**, *343* (6166), 72–6.
- (16) Schnell, O.; Krebs, B.; Carlsen, J.; Miederer, I.; Goetz, C.; Goldbrunner, R. H.; Wester, H. J.; Haubner, R.; Popperl, G.; Holtmannspoter, M.; Kretzschmar, H. A.; Kessler, H.; Tonn, J. C.; Schwaiger, M.; Beer, A. J. Imaging of integrin alpha(v)beta(3) expression in patients with malignant glioma by [18F] Galacto-RGD positron emission tomography. *Neuro-Oncology* **2009**, *11* (6), 861–70.
- (17) Ocampo-Garcia, B. E.; Santos-Cuevas, C. L.; De Leon-Rodriguez, L. M.; Garcia-Becerra, R.; Ordaz-Rosado, D.; Luna-Gutierrez, M. A.; Jimenez-Mancilla, N. P.; Romero-Pina, M. E.; Ferro-Flores, G. Design and biological evaluation of (9)(9)mTc-N(2)S(2)-Tat(49-57)-c(RGDyK): a hybrid radiopharmaceutical for tumors expressing alpha(v)beta(3) integrins. *Nucl. Med. Biol.* **2013**, *40* (4), 481–7.
- (18) Kiessling, F.; Huppert, J.; Zhang, C.; Jayapaul, J.; Zwick, S.; Woenne, E. C.; Mueller, M. M.; Zentgraf, H.; Eisenhut, M.; Addadi, Y.; Neeman, M.; Semmler, W. RGD-labeled USPIO inhibits adhesion and endocytic activity of alpha v beta 3-integrin-expressing glioma cells and only accumulates in the vascular tumor compartment. *Radiology* **2009**, *253* (2), 462–9.
- (19) Wu, Y.; Zhang, X.; Xiong, Z.; Cheng, Z.; Fisher, D. R.; Liu, S.; Gambhir, S. S.; Chen, X. microPET imaging of glioma integrin {alpha}v{beta}3 expression using (64)Cu-labeled tetrameric RGD peptide. *J. Nucl. Med.* **2005**, *46* (10), 1707–18.
- (20) Doss, M.; Kolb, H. C.; Zhang, J. J.; Belanger, M. J.; Stubbs, J. B.; Stabin, M. G.; Hostetler, E. D.; Alpaugh, R. K.; von Mehren, M.; Walsh, J. C.; Haka, M.; Mochtar, V. P.; Yu, J. Q. Biodistribution and radiation dosimetry of the integrin marker 18F-RGD-K5 determined from whole-body PET/CT in monkeys and humans. *J. Nucl. Med.* **2012**, *53* (5), 787–95.
- (21) Ji, S.; Czerwinski, A.; Zhou, Y.; Shao, G.; Valenzuela, F.; Sowinski, P.; Chauhan, S.; Pennington, M.; Liu, S. (99m)Tc-Galacto-RGD2: A novel (99m)Tc-labeled cyclic RGD peptide dimer useful for tumor imaging. *Mol. Pharmaceutics* **2013**, *10* (9), 3304–14.
- (22) Louis, D. N.; Ohgaki, H.; Wiestler, O. D.; Cavenee, W. K.; Burger, P. C.; Jouvet, A.; Scheithauer, B. W.; Kleihues, P. The 2007 WHO classification of tumors of the central nervous system. *Acta Neuropathol.* **2007**, *114* (2), 97–109.
- (23) Liu, S.; Liu, Z.; Chen, K.; Yan, Y.; Watzlowik, P.; Wester, H. J.; Chin, F. T.; Chen, X. 18F-labeled galacto and PEGylated RGD dimers for PET imaging of alphavbeta3 integrin expression. *Mol. Imaging Biol.* **2010**, *12* (5), 530–8.
- (24) Lang, L.; Li, W.; Guo, N.; Ma, Y.; Zhu, L.; Kiesewetter, D. O.; Shen, B.; Niu, G.; Chen, X. Comparison study of [18F]FAI-NOTA-

PRGD2, [¹⁸F]FPPRGD2, and [⁶⁸Ga]Ga-NOTA-PRGD2 for PET imaging of U87MG tumors in mice. *Bioconjugate Chem.* **2011**, *22* (12), 2415–22.

(25) Richards, J.; Miller, M.; Abend, J.; Koide, A.; Koide, S.; Dewhurst, S. Engineered fibronectin type III domain with a RGDWXE sequence binds with enhanced affinity and specificity to human alphavbeta3 integrin. *J. Mol. Biol.* **2003**, *326* (5), 1475–88.

(26) Santra, A.; Kumar, R.; Sharma, P.; Bal, C.; Julka, P. K.; Malhotra, A. F-18 FDG PET-CT for predicting survival in patients with recurrent glioma: a prospective study. *Neuroradiology* **2011**, *53* (12), 1017–24.

(27) Nihashi, T.; Dahabreh, I. J.; Terasawa, T. Diagnostic accuracy of PET for recurrent glioma diagnosis: A meta-analysis. *Am. J. Neuroradiol.* **2012**, *34*, 944–50.

(28) Delbeke, D.; Meyerowitz, C.; Lapidus, R. L.; Maciunas, R. J.; Jennings, M. T.; Moots, P. L.; Kessler, R. M. Optimal cutoff levels of F-18 fluorodeoxyglucose uptake in the differentiation of low-grade from high-grade brain tumors with PET. *Radiology* **1995**, *195* (1), 47–52.

(29) Chen, W. Clinical applications of PET in brain tumors. *J. Nucl. Med.* **2007**, *48* (9), 1468–81.

(30) Tateishi, K.; Tateishi, U.; Sato, M.; Yamanaka, S.; Kanno, H.; Murata, H.; Inoue, T.; Kawahara, N. Application of ⁶²Cu-diacyl-bis(N4-methylthiosemicarbazone) PET imaging to predict highly malignant tumor grades and hypoxia-inducible factor-1alpha expression in patients with glioma. *Am. J. Neuroradiol.* **2013**, *34* (1), 92–9.

(31) Rapp, M.; Heinzel, A.; Galldiks, N.; Stoffels, G.; Felsberg, J.; Ewelt, C.; Sabel, M.; Steiger, H. J.; Reifenberger, G.; Beez, T.; Coenen, H. H.; Floeth, F. W.; Langen, K. J. Diagnostic performance of ¹⁸F-FET PET in newly diagnosed cerebral lesions suggestive of glioma. *J. Nucl. Med.* **2013**, *54* (2), 229–35.

(32) Jeong, S. Y.; Lim, S. M. Comparison of 3'-deoxy-3'-[¹⁸F]fluorothymidine PET and O-(2-[¹⁸F]fluoroethyl)-L-tyrosine PET in patients with newly diagnosed glioma. *Nucl. Med. Biol.* **2012**, *39* (7), 977–81.